第 4 卷 第 2 期
1998 年 5 月

电化学
EL ECTROCHEMISTRY

Vol. 4 No. 2
May 1998

New ESR-Electrochemical Cell Designs for Coaxial Microwave Cavity①

Zhuang Lin * Lu Juntao
(Dept. of Chem., Wuhan Univ., Wuhan 430072)

Abstract New cell designs for simultaneous electrochemical (EC) and electron spin resonance (ESR) measurements are reported for coaxial microwave cavity. Adjustable shieldings are introduced so that the working electrode can be much shorter than the full height of the cavity. Besides the traditional helical electrode, the working electrode can be cylinders made from metal plates, metallic meshes or even composite materials. The counter electrode can be placed either inside or outside the cavity. These features make the new designs more flexible than that previously reported. With a non-perforated cylindrical electrode, this cell can be used to determine the standard potential and the number of electrons of electrode reactions involving radicals. Other possible applications are also briefed.

Key words ESR, Simultaneous electrochemistry, Cell Design

1 Introduction

Since its early stage of development, electron spin resonance (ESR) has been combined with electrochemistry (EC). Simultaneous electrochemical and ESR measurements (SEESR) can be used in different directions and, therefore, are of interdisciplinary interest. Some researchers may use EC as a unique tool for in-situ generation of radicals to study the structure of radicals, the effects of substituents on the molecular orbital energies of a series of related compounds, etc.. Electrochemists may use ESR to detect and study the paramagnetic species involved in electrode reactions. These paramagnetic species may be the intermediate, product or catalyst in an electrode reaction. The charge carrier electrons in conducting polymers and lithium intercalation carbons can also be studied by SEESR measurements.

The cell design is a key to success for SEESR measurements. A good cell design should be

① Received 9 Jan, 1998, Outstanding paper from 9th CES Meeting (1997)

* To whom correspondence should be addressed

able to meet the conditions necessary for both normal ESR measurements and electrochemical operations. However, the conditions required by the two sides are often in conflict to some extent. On one hand, a highly conductive electrolyte solution favored by electrochemical operations inevitably tends to cause serious dielectric loss to the ESR cavity. On the other hand, in order for the ESR measurement to be conducted normally, the volume of the SEESR cell is severely limited and the cell shape must meet some special requests. For a rectangular ESR cavity, the available space for the SEESR cell is about 1 cm wide with the maximum length equal to the height of the cavity and a thickness no more than 0.5 mm. For cylindrical cavity, the effective volume of the cell is a cylinder of 1~2 mm diameter along the axis of the cavity. As a result, most of the reported cell designs fall into two basic categories, i.e., flat cells and capillary cells, to fit the two cavities respectively.

A properly designed cell not only must exhibit performance that is considered satisfactory for a particular experiment but should be easy to make and operate. There have been a variety of designs reported in the literature and collected in review papers in different periods[1-3]. Each cell design has its merits and shortcomings and is applicable to a wider or narrower range of experimental parameters, such as the dielectric constant of the solvent, the concentration of paramagnetic species, the required precision of potential control over the working electrode, the duration of undistorted semifinite diffusion mode, the time constant for exhausting electrolysis, etc.. In this paper, we report new cell designs based on the coaxial microwave cavity concept with an emphasis on improving the flexibility and applicability.

The first cell design based on the concept of coaxial microwave cavity was reported by Allendoerfer and coworkers[4]. In their design the working electrode is a finely wound metal helix fitted snugly against the inner wall of an ESR sample tube of 6 mm inner diameter. The length of the helix is somewhat longer than the height of the cylindrical cavity (about 4.4 cm for x-band microwave). The counter electrode is located in the center of the helix while the Luggin capillary for the reference electrode is placed close to the inner surface of the helix. The ESR observable space is confined to the volume between the metal helix and the inner wall of the sample tube. This design has some obvious advantages. This cell can be used for a wide range of solvents with different dielectric constants, from water to organic solvents. The potential over the whole working electrode surface can be fairly uniformly controlled because of the symmetric arrangement of the electrodes; the distortion of voltammogram due to IR drop is negligible; the paramagnetic species generated at the counter electrode is screened from ESR detection by the metal helix; the time for exhausting electrolysis is relatively short (about 30 seconds); the large surface area of the working electrode makes it advantageous to detecting short-lived radicals. The performance of the cell seems very attractive; however, the long and finely wound helical electrode is not convenient to deal with, especially when the sample tube is thinner. For example, for a conventional ESR sample tube of 4 mm inner diameter, a 4.4 cm finely wound helix made from a metal wire of 0.3

mm diameter has over a hundred turns and needs about 1.5 meters of wire. It is not an easy job to make such a component in common laboratories. Besides, in some experiments, the electrode surface has to be cleaned mechanically. In these cases, repeated unwinding and winding the helix become necessary and these would easily cause a break to the wire, which is often made from noble metals and costly. The purpose of this work was to try to modify the orginal design so that the SEESR cell could be prepared easier and more flexible to suit wider range of experiments.

2 Cell design

In Allendoerfers' design, the helix wire has two functions. In addition to being a working electrode, it shields the most part of the solution in the cell from the microwave radiation to avoid severe dielectric loss. To be a working electrode, a full-length (the height of the ESR cavity) helix is not necessary though a long helix means a big electrode surface area favorable for the sensitivity of ESR detection. In many cases, the sensitivity is not a major concern and a mush shorter helix electrode may still generate sufficient number of radicals for ESR measurements. A shorter helical electrode is obviously easier to handle. To ensure an acceptable dielectric loss, however, the helix must be full length in Allendoerfer's design to shield most part of the solution.

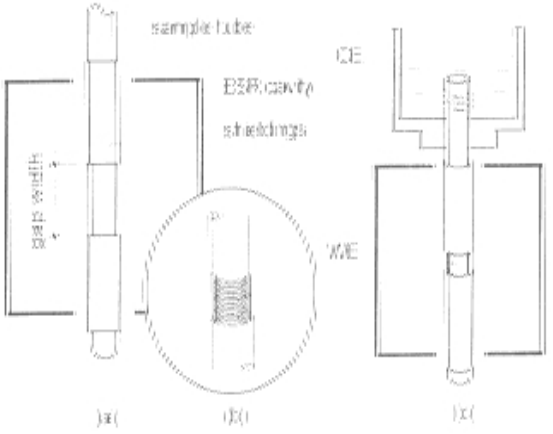

Fig. 1 The cell design. (a) the SEESR cell with adjustable shieldings; (b) an enlarged view of a short helical working electrode with shieldings; (c) the cell with the counter electrode placed outside the cavity

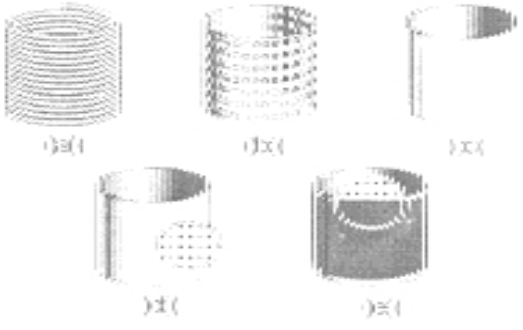

Fig. 2 Examples of the working electrode for the coaxial cavity. (a) helix; (b) perforated cylinder; (c) non-perforated cylinder; (d) metallic mesh; (e) carbon sheet-metallic mesh composite

In the new design, a part of the shielding function of the helix is taken over by two adjustable metal shieldings so that the working electrode can be much shorter. The adjustable shieldings are made from highly conducting metal (Ag, Cu or Al) foils by simply wrapping the foils round the ESR sample tube and fixing them with adhesive tape (Figure 1a). Experiments show that it is important to have the outside surface of the metal shields polished bright. The two shielding cylinders can be moved up and down on demand. The gap between them is centered in

the cavity. The length of the working electrode just fills up the gap. In this way, the helix can be mush shorter than the cavity height. Besides the wound metal wire, the working electrode may be a cylinder made from different materials, such as perforated or non-perforated metal foils, metallic mesh or even composite sheets (Figure 2).

In most experiments reported in this paper, the counter electrode was a platinized thick Pt wire located in the center of the cell along the axis of the helix. A roughened silver wire sealed in a thin Teflon tube served as the reference electrode. Another thin Teflon tube was inserted down to the cell bottom for purging the solution with argon.

In prolonged experiments, the product formed at the counter electrode may eventually reach the working electrode through conventional diffusion and cause interference to the SEESR measurements. In these cases, the counter electrode can be moved outside the cavity as shown in Figure 1c. In this design, the conventional mass transport for the species formed at the counter electrode is limited by the special configuration. If the density of the product at the counter electrode is lower than that of the bulk solution, it will rise up and float at the top of the solution; if the density is higher than that of the bulk solution it will sink down and stay at the bottom of the upper container outside the cavity. The long distance between the counter and the working electrodes makes it practically impossible for the products to diffuse from the counter electrode to the working electrode. Thus, the interference caused by the product at the counter electrode can be effectively avoided. This advantage is obviously obtained at the expense of the uniformity of potential distribution over the working electrode. For a given electrochemical system, the potential non-uniformity due to ohmic drop is determined by the ratio of the electrode length and the cross-section area of the electrolyte channel in contact with the electrode. In this connection, the design in Figure 1c is still better than the widely cited flat cell[5]. To give an impression of the IR effects of this cell, here we present a set of cyclic voltammograms obtained with 1 m mol/L $Fe(CN)_6^{3-/4-}$ in 0.5 mol/L KCl (Figure 3). The peak potential separations for scan rates 1, 10, 40 and 100 mV/s are approximately 40, 70, 90 and 105 mV, respectively. The peak separation 40 mV for the slowest scan is smaller than the typical value for a one-electron reversible system, 59 mV. This was caused by the thin layer effect, which is characteristic for all the coaxial cell designs mentioned in this paper and will be discussed below in more detail.

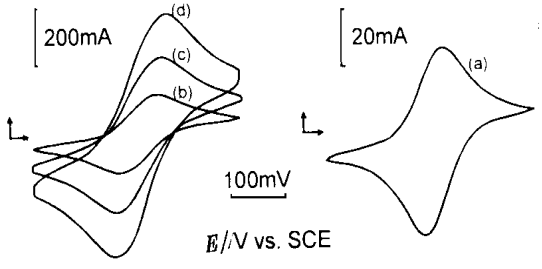

Fig. 3 Cyclic voltammograms obtained with the cell design shown in Figure 1c for 1 m mol/L $Fe(CN)_6^{3-/4-}$ in 0.5 mol/L KCl at scan rates (mV/s) a) 1, b) 10, c) 40 and d) 100

3 Experimental

Instrumentation and methods

ESR measurements were conducted on JEOL JES-FE1XG ESR spectrometer with TE_{011} cylindrical cavity working at X-band. A Mn(Ⅱ) marker was kept in the cavity to serve as both the indicator for the Q-factor of the cavity and the inner scale for the mangetic field. The electrochemical system consisted of a Pine AFRDE 5 bipotentiostat and YEW 3036 x-y recorder. All experiments were performed at room temperatures. The potentials are reported with respect to SCE.

To test the effectiveness of the adjustable shieldings and the influence of the gap width on ESR signal measurements, ESR intensity was measured as a function of the gap width using 4-hydroxyl-TEMPO (2,2,6,6-tetramethyl piperidine oxyl-1, Sigma) solution as the sample. To demonstrate the performance of the cell, simultaneous ESR and electrochemical measurements were carried out using methylviologen (MV, BDH Chemicals) as a model system. Modifications in cell configuration were made in some individual applications and additional experimental details will be given in relevant sections below.

4 Results and discussion

The behaviors of the helical electrode in the presence of the adjustable shieldings were essentially identical to that of the full-length helical electrode as reported by Allendoerfer, except for the variable sensitivity depending on the gap width. Therefore, we here only report and discuss the results associated with the new features of the cell designs, including the effects of the adjustable shieldings and the performance of different working electrodes. Besides, the thin layer effect that was overlooked in previous papers will also be discussed.

The effects of the adjustable shieldings

Figure 4a shows the ESR intensity, I_{ESR}, measured at different gap widths between the two shielding cylinders. The gap was centered in the ESR cavity and a full length helix made of silver wire of 0.3 mm diameter was snugly fitted the inside wall of a conventional ESR tube (inner diameter 4 mm) filled with an aqueous solution of 4-hydroxyl-TEMPO (ca. 1 m mol/L). The ESR intensity obtained without the shieldings is used as the basis for normalization in Figure 4a. Curve 1 shows that ESR intensity increases with increasing gap width first and then reaches a maximum located about 3/4 of the full length.

The shape of curve 1 in Figure 4a is thought to be determined by two factors, the number of the radicals exposed to the microwave radiation and the Q-factor of the cavity. Curve 4 is the Q-factor as a function of the gap width, normalized to the value for the full-length gap width. The relative values of Q-factor were calculated from the ESR intensities of the Mn marker. After correction for the changes in the Q-factor, curve 1 becomes curve 2.

Figure 4b is the normalized ESR intensity of a small sample at different location along the ax-

is of the cavity. These data can also be regarded as the ESR sensitivity distribution along the axis. The data points were obtained using a DPPH (diphenylpicrylhydrazyl) sample as a probe. A small amount of DPPH was applied to a ring made of a narrow (about 1 mm wide) strip of filter paper that was fixed round an empty ESR sample tube. The sample tube was then put in the cavity along the cavity axis for ESR measurements. Caution was taken to ensure that the whole height of the cavity was filled with the ESR tube to keep the Q-factor constant. As shown in Figure 4b, the data points fit well the theoretical curve $\cos^2(\pi x/h)$ (solid line in Figure 4b) for the microwave intensity distribution in the cavity[3], where x is the distance from the cavity center along the cavity axis and h is the height of the cavity. Curve 3 in Figure 4a is the normalized integrated ESR sensitivity which is represented by the shadowed area in Figure 4b for a given gap width. The reasonable agreement between curves 3 and 2 in Figure 4a confirms the above mentioned two main factors governing curve 1 in Figure 4a. The slight difference between curves 2 and 3 in Figure 4a may be attributed to some distortion of microwave field due to the insertion of the electrochemical cell.

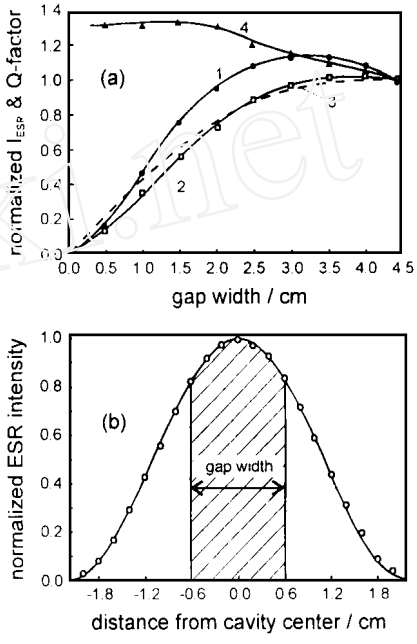

Fig. 4 Influence of gap width on ESR measurements. (a) Normalized ESR intensities and Q-factors *vs*. gap width: 1, measured ESR intensity; 2, ESR intensity after correction for Q-factor changes; 3, ESR intensity calculated from b; 4, normalized Q-factor. (b) Normalized ESR intensity for a ring sample located at varying height in the cavity (open circles) and the theoretical curve $\cos^2(\pi x/h)$ (solid line)

It is interesting to note the favorable features of curve 1 in Figure 4a. Its maximum at the gap width 3 cm is about 13 % higher than the ESR intensity of the full length helical electrode. Besides, the intensity of a full length helical electrode can be reached by using an electrode of only a half of the full length with the shieldings present. Curve 1 in Figure 4a provides a guideline to determine the gap width suitable for concrete experimental conditions. When the concentration of electrochemically generated radicals is high the gap width can be made small, say a few millimeters. If a helical electrode is to be used, it will be much easier to deal with such a short helix than a full length one.

SEESR measurements with a perforated cylindrical electrode

To test the feasibility of the perforated cylindrical electrode as a replacement for the helical electrode, a silver cylinder was made from a piece of 0.1 mm thick Ag plate. The holes in the plate had a diameter 0.3 mm and were arranged in about 0.9 mm ×1 mm array (Figure 2b).

Figure 5 shows the cyclic voltammogram for the redox reactions of methylviologen in 0.5 mol/L KCl aqueous solution and the simultaneously recorded ESR intensity at a fixed magnetic field. The two cathodic peaks correspond to the two steps of one-electron charge transfer:

peak Ⅰ　　$MV^{2+} + e^- \rightarrow MV^{+\cdot}$　　(A)

peak Ⅱ　　$MV^{+\cdot} + e^- \rightarrow MV$　　(B)

Peak Ⅰ and the corresponding anodic peak are centered round - 0.69 V (vs. SCE) with a peak separation about 40 mV. This peak separation is smaller than the standard value 59 mV (25 ℃) for a reversible redox couple in solution under semi-infinite diffusion condition. The observed smaller peak separation may be attributed to the fact that the cell configuration bares the characteristics of a thin-layer cell to some extent. The space between the working electrode and the sample tube wall forms a thin layer of solution that can exchange solutes with the bulk solution only through the holes. The other side of the working electrode facing the center of the sample tube can be considered to be under semi-infinite diffusion condition. The observed current is actually the sum of the currents generated at both sides of the working electrode. For a typical thin-layer cell, the peak separation for reversible redox couples is zero, resulting from a homogeneous consumption of the dissolved reactants in the whole thickness of thin-layer solution. This happens only if the potential scan rate is sufficiently slow. In our experiment, the condition was far from that of a typical thin-layer cell but bore some influence of the thin-layer effect. When potential scan rate is increased, this effect became less noticeable. For example, the peak separation increased to 60 mV at scan rate 200 mV/s.

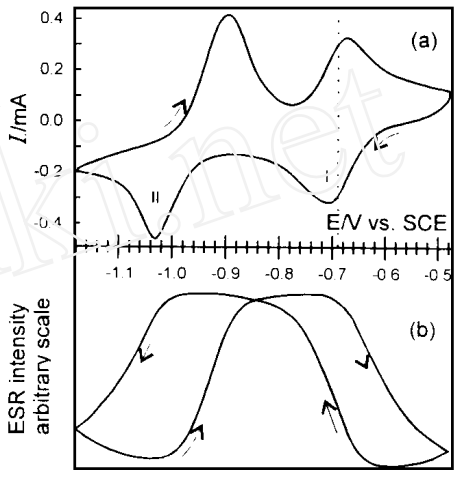

Fig. 5　SEESR measurements with a perforated Ag cylindrical electrode for 1 m mol/L MV + 0.5 mol/L KCl aqueous solution, potential scan rate 10 mV/s. (a) Cyclic voltammetry; (b) ESR intensity as a function of potential

The thin-layer effect can be regulated by changing the hole density. With increasing hole density the solution confined between the working electrode and the tube wall becomes less isolated from the bulk solution in terms of mass transport, resulting in a decrease in the thin-layer effect. Conversely, a decrease in hole density will make the thin-layer effects more prominent. Our experiments have proved that the thin-layer effect also exists with the helical electrode if the space between the turns is small and potential scan is slow. While the thin-layer effect may be annoying for obtaining a perfect voltammogram, it is useful in some other cases. For example, the thin-layer cell with an optical transparent electrode has been widely used for determining the standard potential of redox couples[6]. A demonstration of an ESR analog with a cylindrical working electrode

is given below.

Non-perforated cylindrical electrode used as a thin-layer electrode

The most popular application of the potical spectroelectrochemistry with a thin-layer cell is to determine the standard (or formal) potential of a redox couple and the number of electrons involved. The cylindrical ESR electrode provides an excellent analog for vedox couples involving radiculs. In our experiment, the time of exhausting electrolysis for the thin layer solution between the cylindrical electrode and the ESR tube was well below 30 seconds. As a demonstration, data for the MV^{2+}/MV^{+} couple are given in Figure 6. The cylindrical Ag electrode used in this measurement was not perforated and had a height of 2.5 cm. The gap between the two shieldings was 1 cm. The upper and lower edges of the working electrode were covered with the shileldings to prevent the interference of edge effects. The electrode potential was controlled potentiostatically point by point, while the peak-to-peak height of a selected spectral band was taken as the ESR intensity, I_{ESR}. According to the Nernst equation,

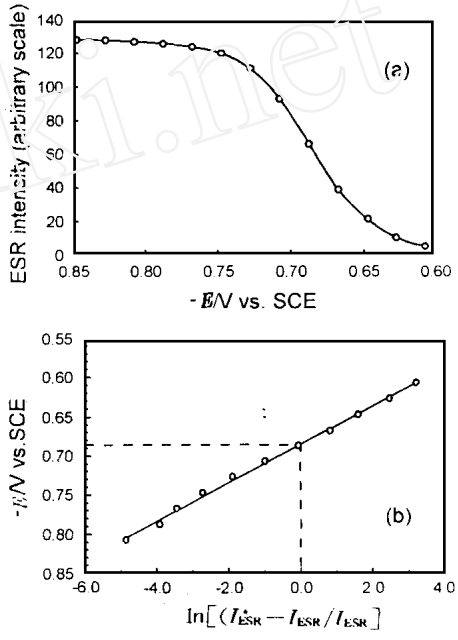

Fig. 6 Steady state thin-layer behavior of the cylindrical electrode for MV. (a) I_{ESR} v E; (b) $\ln[(I^{*}_{ESR} - I_{ESR})/I^{*}_{ESR}]$ vs E

$$E = E^{0} + (RT/nF)\ln[(I^{*}_{ESR} - I_{ESR})/I_{ESR}] \quad (1)$$

where R is the gas constant, T and F are the absolute temperature and the faradaic constant and n is the electron number involved in the reaction; I_{ESR} and I^{*}_{ESR} are the ESR intensity and its maximum value recorded at the negative extreme of the potential region studied. It can be seen from Figure 6b that there is a good linearity between $\ln[(I^{*}_{ESR} - I_{ESR})/I_{ESR}]$ and E, showing $n = 1$ and $E^{0} = -0.685$ V (vs. SCE). These results are in good agreement with the characteristics of the cyclic voltammogram (Figure 5) and the data reported in literature[7].

Other applications

The cell designs reported in this paper can be applied to a wide range of SEESR studies. Besides the demonstrative experiments described above, we have used perforated cylindrical electrode successfully to do potential modulated SEESR[8] and to study conducting polymers[9]. In the work of potential modulated SEESR, the electrode was coated with Nafion which had to be removed from the electrode mechanically after each measurements. We found it much easier to remove Nafion coating mechanically from the perforated cylinder than from a helix. In another experiment, the SEESR measurement for Li intercalation into carbon, the new design became even

more important. In a previous paper, we reported the determination of the density of states at the Fermi level in carbon as a function of the extent of Li intercalation[10]. In principle, one can process the data further to separate the so-called ionic and electronic factors governing Li intercalation[11]. This separation is important to gain a deeper insight into the structure-function relations for Li intercalation carbons but has never been realized because of a lack of suitable experimental techniques. The shortcoming of the SEESR cell (the sandwich type) used in the previous work was that the SEESR could be conducted only for the first Li intercalation (charging) process. Unfortunately, in the first intercalation process, only a part of the electricity is consumed for Li intercalation. This makes it impossible to process the data for separating the two factors. Therefore, it is necessary to do SEESR in the successive charging-discharging cycles. However, during the deintercalation (discharging) process of the carbon electrode, fine Li particles formed at the counter electrode and caused a huge interfering ESR signal, discouraging further measurements. In the new design, we use the composite working electrode (Figure 2e). The counter electrode is placed in the center of the working electrode and is shielded from ESR observation so that SEESR measurements for the second and successive charging-discharging cycles have become possible. The experiment is in progress and will be reported elsewhere.

5 Conclusion

New cell designs based on coaxial cavity concept are reported and demonstrated with applications to a few systems. With the adjustable shieldings, the length of the working electrode is no longer necessarily full length (the height of the cavity) and can be varied according to the concrete experimental conditions. The working electrode can be either a traditional metallic helix or a cylinder made of metal plates (either perforated or non-perforated), meshes or even composite materials. The counter electrode can be either inside or outside the ESR cavity. These new features provide much flexibility for SEESR experiments and are expected to find wide applications.

Acknowledgement The authors are grateful to the National Natural Science Foundation of China for financial support to this work.

References

1 McKinney T M. Electron Spin Resonance and Electrochmistry. Electroanalytical Chemistry, Vol. 10, ed. Bard A J. Dekker M. New York, 1965, chap. 2

2 Kastening B. Electron Spin Resonance. Comprehensive Treatise of Electrochemistry, vol. 8, ed. White R E, Bockris J O'M, Conway B E. New York: Plenum Press, 1984, chap. 7

3 Goldgerg I B, McKinney T M. Principles and Techniques of Electrochemical-Electron Paramagnetic Resonance Experiments. Laboratory Techniques in Electroanalytical Chemistry, ed. Kissinger P T, Heineman W R, Dekker M. New York: 1996, chap. 29

4 Allendoerfer R D, Martinchek G A, Bruckenstein S. Simultaneous Electrochemical-Electron Spin Resonance Measurements with a Coaxial Microwave Cavity. Anal. Chem., 1975, 47: 890
5 Goldgerg I B, Bard A J. Simultaneous Electrochemical-Electron Spin Resonance Measurements. I. Cell Design and Preliminary Results. J. Phys. Chem., 1971, 75: 3 281
6 Hawkridge F M, Kuwana T. Indirect Coulometric Titration of Biological Electron Transport components. Anal. Chem., 1973, 45: 1 021
7 Bird C L, Kuhn A T. Electrochemistry of the Viologens. Chem. Soc. Rev., 1981, 10: 49
8 Zhuang L, Lu J. Development in potential-modulated ESR technique. J. Electroanal. Chem., 1997, 429: 115
9 Mu S, Kan J, Zhuang L, Lu J. Interconversion of polaron and bipolaron of polyaniline during the electrochemical polymerization of aniline. J. Electroanal. Chem., in press
10 Zhuang L, Lu J, Ai X, Yang H. In-situ ESR study on electrochemical lithium intercalation into petroleum coke. J. Electroanal. Chem., 1995, 397: 315
11 Gerischer H, Decker F, Scrosati B. The Electronic and the Ionic Contribution to the Free Energy of Alkali Metals in the Intercalation Compounds. J. Electrochem. Soc., 1994, 141: 2 297

新型 ESR—电化学池设计①

庄 林* 陆君涛
(武汉大学化学系 武汉 430072)

摘要 本文报道了一种适用于同轴微波腔的新型 ESR—电化学池的设计。工作电极的长度可调节,部分屏蔽微波辐射的功能由上下两个屏蔽套承担。除了传统的螺线管,工作电极还可由打孔的金属筒、金属网、甚至复合材料制成。对电极可根据需要置于共振腔的外面或里面。总之,新设计灵活实用,适合更多的研究场合。本文列举了一些应用实例。

关键词 ESR,同步电化学,电化学池设计

① 第九次全国电化学会议(1997)优秀论文